PORE STRUCTURE OF VUGGY CARBONATES AND RATE DEPENDENT DISPLACEMENT IN CARBONATE ROCKS

Neeraj Rohilla, Dr. George J. Hirasaki

Dept. of Chemical and Biomolecular Engineering, Rice University, Houston, TX 77005

This paper was prepared for presentation at the International Symposium of the Society of Core Analysts held in Austin, Texas, USA 18-21 September, 2011

ABSTRACT

The carbonate samples which are focus of this study are brecciated and fractured. In order to characterize the pore size in vuggy carbonates, we use NMR along with tracer analysis. The distribution of porosity between micro and macro-porosity can be measured by NMR. Tracer analysis is used to characterize the pore structure by estimating flowing fraction, dispersivity and mass transfer coefficient between flowing and stagnant streams.

For heterogeneous samples, we have found that permeability value differs by two orders of magnitude (2 mD and 210 mD) for 1.5 inch diameter and 3.5 inch diameter samples respectively. Flowing fraction is estimated to be 0.25-0.5. For most samples mass transfer between flowing and stagnant streams is very poor. Tracer experiments suggest that at moderate flow rates (1-10 ft/day) only a small fraction of matrix is contacted by flowing stream even after five pore volumes. Based on this, the rate of surfactant flood required for optimum contacting between flowing and stagnant streams can be calculated for enhanced recovery of oil.

INTRODUCTION

More than 50 % of the world's hydrocarbons are contained in carbonate reservoirs [1]. Accurate characterization of pore structure of carbonate reservoirs is essential for design and implementation of enhanced oil recovery processes. However, characterizing pore structure in carbonates is a complex task due to the diverse variety of pore types seen in carbonates and extreme pore level heterogeneity.

Carbonate reservoirs have complex structures because of depositional and diagenetic features. Carbonates may contain not only matrix and fractures but also vugs. A vug can be defined as any pore that is significantly larger than a grain or inside of a grain. Vugs are commonly present as leached grains, fossil chambers, fractures, and large irregular cavities. Vugs are irregular in shape and vary in size from millimeters to centimeters. Vuggy pore space can be divided into separate-vugs and touching-vugs, depending on vug interconnection. Separate vugs are connected only through interparticle pore

networks and do not contribute to permeability. Touching vugs are independent of rock fabric and form an interconnected pore system enhancing the permeability [1].

SAMPLE PREPARATION AND CHARACTERIZATION

Core samples for experiments were cleaned using a bath of Tetrahydrofuran (THF) followed by Chloroform and Methanol. Core-plugs were dried overnight in the oven at 80^0C. Core-plugs were wrapped in heat shrink tubing to protect against wear and tear and chipping away of the sharp edges. After cleaning, core-plugs were saturated with 1% NaCl brine solution using vacuum saturation followed by pressure saturation at 1000 psi for 24 hours. Before performing NMR experiment, core-plug was wrapped in paraffin film to avoid the gravity drainage of brine solution from big vugs.

NMR Results: NMR experiments were performed on 100% brine saturated core-plugs on 2 MHz Maran-SS. Only 1.5 inch diameter plugs were used in the experiments because the NMR instrument cannot accommodate 3.5 inch diameter plugs. For experiments, half-echo spacing of 200 μs was used and signal to noise ratio of 100 was used.

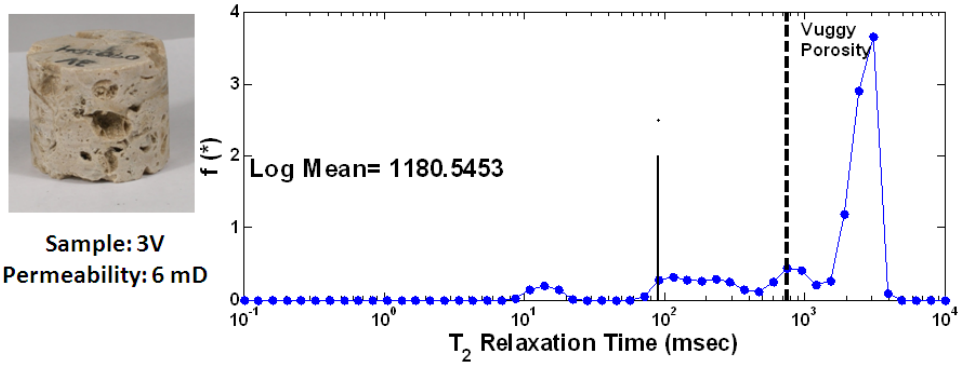

Figure 1. T_2 relaxation time spectrum of 100% brine saturated rock sample for core sample: 3V

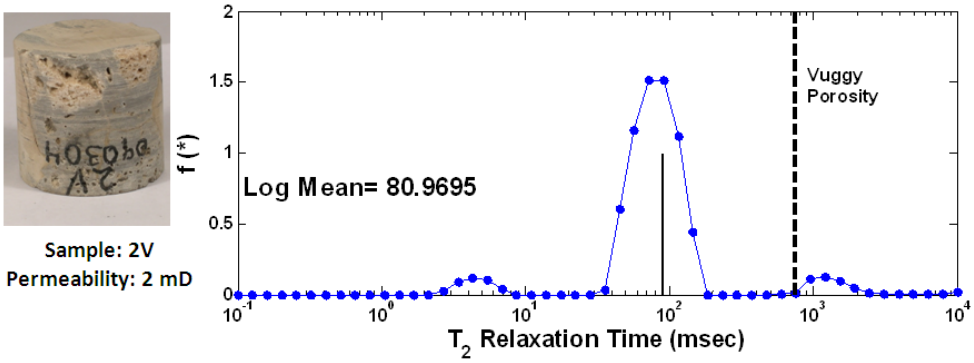

Figure 2. T_2 relaxation time spectrum of 100% brine saturated rock sample for core sample: 2V

Figures 1-5 show T_2 relaxation time spectrum for various core plugs taken from different source rocks. Black solid vertical line corresponds to the traditional cutoff value of 90 ms for carbonate rocks. The dashed vertical line separates the relaxation spectrum into non-vuggy and vuggy porosity by assuming that T_2 values of 750 ms and higher correspond to vugs [2]. The permeability values for the majority of the core plugs are within the range of 0.5-6 mD. Figure 1 shows that for core plug 3V majority of the porosity resides in these large vugs and contribution of small pore sizes to porosity is very small. NMR response for core plug 2V (Figure 2) shows the peak at relaxation time of about 90 ms. Using the traditional cut off formula would classify 2V sample as non-pay. The low value of permeability suggests that the vugs do not form an interconnected pore network.

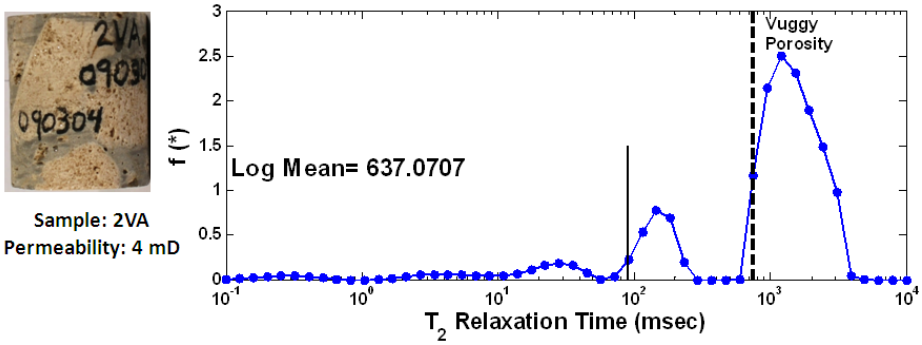

Figure 3. T_2 relaxation time spectrum of 100% brine saturated rock sample for core sample: 2VA

Figure 3 shows the T_2 relaxation time spectrum for a core plug 2VA. Although, this plug was drilled from the same source rock as the previous sample (Figure 2), NMR response shows a large contribution from vugs and relatively smaller contribution from small sized pores. Figure 4 and 5 show the T_2 relaxation time spectrum for core plugs 1H and 1HA. In both cases, we observe that relaxation time has contributions from small sized micro-pores, vugs and some intermediate size pores. The low value of permeability suggests that vugs are isolated vugs and do not create any interconnected flow channels.

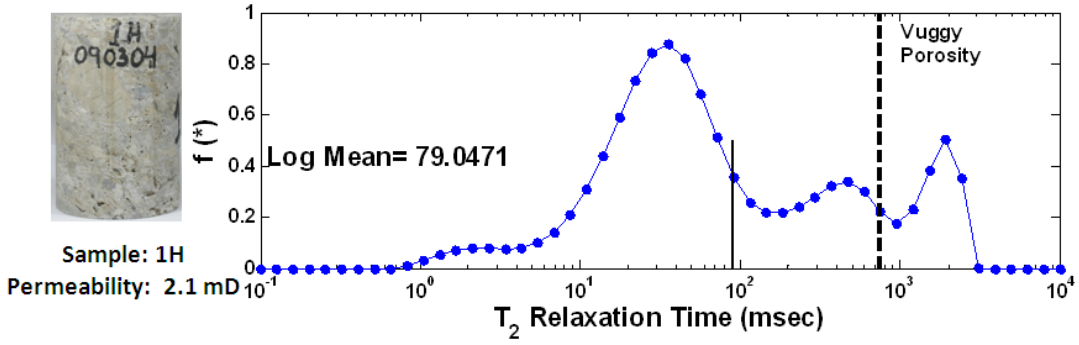

Figure 4. T_2 relaxation time spectrum of 100% brine saturated rock sample for core sample: 1H

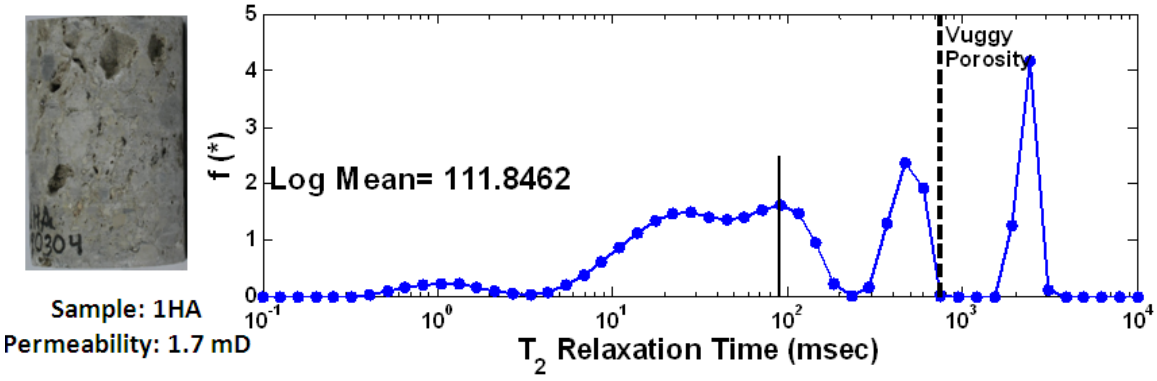

Figure 5. T_2 relaxation time spectrum of 100% brine saturated rock sample for core sample: 1HA

Table 1 summarizes T_2 log mean and measured values of permeability for various core plugs. NMR results suggest that these carbonate rocks are very heterogeneous. In some cases, vugs contribute most to the porosity while in other smaller pores are dominant. Samples taken within the proximity of 3 inches exhibit very different T_2 relaxation time spectrum. Most of the samples show small value of permeability and there is no obvious correlation with the value of T_2 Log mean.

Table 1. T_2 Log mean versus permeability for various core plugs

S. No.	Core ID	T2 Log Mean (ms)	Permeability (mD)
1	3V	1180	6
2	2V	81	2
3	2VA	637	4
4	1H	79	4
5	1HA	112	1.7
6	6H	436	45
7	6HA	-	510
8	8V	247	3
9	9V	140	2

TRACER ANALYSIS

In this section, we describe methods to characterize the key features of pore structure such as fraction of dead-end pores and dispersion and capacitance effects. We use the modified version of differential capacitance model of Coats and Smith [3] and a solution procedure developed by Baker [4] to study dispersion and capacitance effects in cores. Brigham [5] showed that differential capacitance model can be written for either flowing (effluent) concentration or in-situ concentration. During tracer experiments, flowing concentrations are measured hence in the following formulation we work with flowing (effluent) concentrations. The differential capacitance model assumes:

1. The fluid flow is one dimensional
2. The fluid flow is single phase flow

3. The fluid and porous media are incompressible
4. The fluid density is constant
5. The porosity is constant throughout the system

The model can be described by the following set of differential equations:

$$f\frac{\partial C}{\partial t} + (1-f)\frac{\partial C^*}{\partial t} = K\frac{\partial^2 C}{\partial x^2} - \frac{u}{\Phi}\frac{\partial C}{\partial x} \quad (1)$$

$$(1-f)\frac{\partial C^*}{\partial t} = M(C - C^*) \quad (2)$$

The domain of interest is: x > 0

Where, ***K*** is dispersion coefficient, **(1-*f*)** is the fraction of dead end pores, **Φ** is the porosity, ***M*** is the mass transfer coefficient, ***C*** is tracer concentration in flowing stream, C^* is the tracer concentration in stagnant volume and ***u*** is the superficial velocity. Interstitial velocity ***v*** can be defined as, $v = \frac{u}{\Phi}$.

The boundary and initial conditions are:

$$C(0,t) = C_{BC} \quad (3)$$

$$C(\infty,t) = C_{IC}$$

$$C(x,0) = C_{IC}$$

$$C^*(x,0) = C_{IC}$$

$\mathbf{c_{BC}}$ is injected concentration at the inlet (x=0) and $\mathbf{c_{IC}}$ is the initial concentration in the system at the start of the experiment (t=0). The governing and boundary and initial conditions are made dimensionless as follows: $\hat{x} = \frac{x}{L}$, $\hat{t} = \frac{t}{t_0}$, $t_0 = \frac{L}{v}$; where v is the interstitial velocity ($v = \frac{u}{\Phi}$) and L is system length. Dimensionless concentrations are defined as:

$$\hat{C} = \left(\frac{C - C_{IC}}{C_{BC} - C_{IC}}\right) \text{ and } \hat{C}^* = \left(\frac{C^* - C_{IC}}{C_{BC} - C_{IC}}\right)$$

Using the above mentioned dimensionless variables the system is characterized by three dimensionless groups which are defined as follows.

$$f, N_K = \frac{K}{Lv} = \frac{\alpha}{v} \text{ and } N_M = \frac{ML}{v}$$

f is the flowing fraction, N_K is similar to the inverse of macroscopic Peclet number and N_K is the ratio of dispersivity to system length. N_M defines the ratio of the rate of mass transfer to the rate of convection. The above set of differential equations with gives

boundary and initial conditions can be solved using Laplace transform. The solution can be expressed in terms of dimensionless Laplace variable as follows:

$$\mathcal{L}(\hat{C}) = \left(\frac{1}{\hat{s}}\right) exp\left[\left(\frac{\hat{s}}{2N_K}\right)\left(1 - \sqrt{1 + 4N_K\hat{s}\left(f + \frac{N_M}{\hat{s}+\frac{N_M}{1-f}}\right)}\right)\right] \quad (4)$$

The resulting solution can be numerically inverted into time domain using the computer program of Hollenbeck [6] which is based on the algorithm of De Hoog, Knight and Stokes [7]. Baker [4] and Salter et. al [8] suggested that rather than transforming equation 4 into time domain for the purpose of parameter estimation, the experimental data should be transformed into the Laplace domain for obtaining fitted parameters using least square curve fitting. The fitted parameters correspond to a set which minimizes the error. Parameter estimation is done by using Lavenberg-Marquardt algorithm [9]. When the value of $\mathbf{N_M}$ is large, the fitted parameters may not be correct due to non-uniqueness of the solution. This happens because large value of mass transfer coefficient allows of exchange between stagnant and flowing stream and resulting fitted parameters show apparent higher value of flowing fraction. To obtain unique set of parameters, we use experimental data of effluent concentration at two different flow rates. We further assume that mass transfer between stagnant and flowing streams is dominated by diffusion coefficient and mass transfer coefficient does not depend on the flow rate. The dispersion coefficient ($\boldsymbol{K}$) varies linearly with interstitial velocity ($\boldsymbol{v}$). We use these additional constraints in the cost function of parameter estimation algorithm and obtain fitted model parameters for two cases simultaneously.

The rock samples subject of this study are heterogeneous in nature and some of the assumptions of Coats and Smith model (constant porosity and one dimensional flow) may not be completely satisfied.

Recovery Efficiency and Transfer Between Flowing And Stagnant Streams

Tracer flow analysis described in previous section can be complimented with the help of recovery efficiency calculations. Recovery efficiency is defined as the fraction of initial fluid in place displaced with injected tracer fluid.

$$\text{Recovery Efficiency} = \int_0^{\hat{t}_{max}} (1-\hat{C})d\hat{t}$$

Hence, recovery efficiency can be plotted as a function of pore volume throughput. When all of the initial fluid in place is displaced by injected tracer fluid, the recovery efficiency approaches unity. Two sets of synthetic datasets shown in figure 6 have same value of flowing fraction and dispersivity (α) but different values of mass transfer group (N_M). In first case even though the effluent concentration approaches unity after 1.5 pore volumes,

the recovery efficiency is only 0.4 and hence most of initial fluid in place has not been replaced by injected tracer fluid. Larger value of N_M in second case results in significant mass transfer between flowing and stagnant streams and recovery efficiency approaches unity after about 2 pore volumes. Hence, recovery efficiency is an excellent measure of the fraction of dead end pores contacted by displacing tracer fluid.

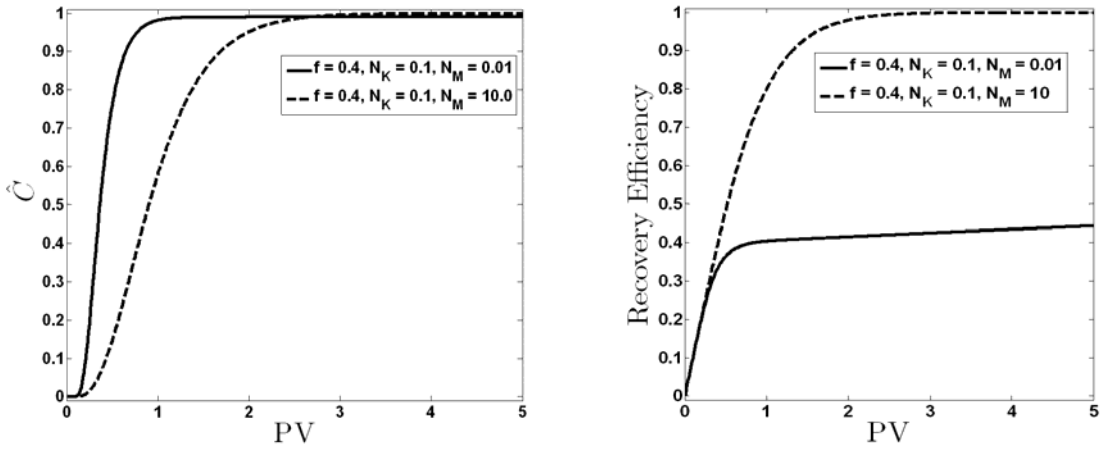

Figure 6. Plots of effluent concentration and recovery efficiency as a function of pore volume throughput illustrating importance of mass transfer between flowing and stagnant streams

Setup For Tracer Experiments

The core holder for 1.5 inch diameter samples is Hassler type core holder. We have adopted similar design for fabricating flow setup for 3.5 inch diameter core samples. Based on NMR results and permeability measurements, we believe that larger diameter samples are better candidates to study the connectivity of vugs and to accurately characterize the pore structure.

Sodium bromide is used as tracer in the experiments. For experiments, the initial tracer concentration is 100 ppm and injected tracer boundary condition is 10,000 ppm To measure the tracer concentration at outlet, a bromide ion sensitive electrode is used in combination with a flow cell. Bromide electrode and flow cell enable us to measure tracer concentration continuously without collecting multiple effluent samples and analyze them separately.

TRACER FLOW EXPERIMENTS

Validation with Sandpack Systems: Two types of sandpack systems are used in tracer experiments. The length of sandpack systems is about one feet. Homogeneous sandpack is prepared by using a single sand layer which has fairly uniform particle size distribution. Heterogeneous sandpack consists of two layers of sand. The top layer sand is of low permeability and the bottom layer sand has a permeability value which is 19 times that of the top layer. Each sand layer occupies half of the volume in the sand pack. This system represents a case where the flowing fraction would be less than one and there will

be significant mass transfer between stagnant and flowing streams. Figure 12 shows the plot of effluent concentration versus pore volume throughput for both homogeneous and heterogeneous sandpacks. Figure 7 shows early breakthrough of tracer which is a measure of smaller flowing fraction. We also notice that effluent concentration increases slowly after an early breakthrough. The flowing fraction for this case was interpreted to be about 0.65 from effluent concentration data.

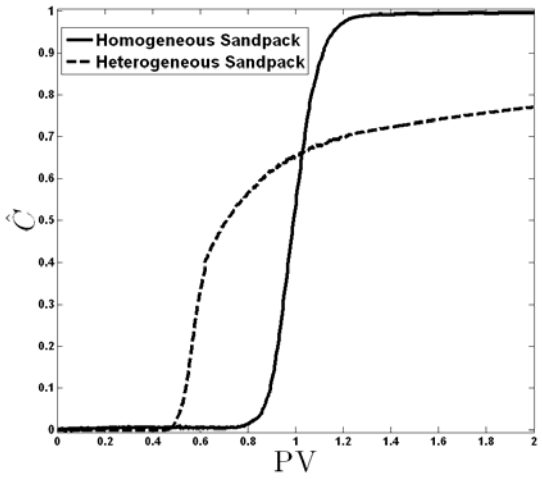

Figure 7. Effluent concentration versus pore volume throughput for homogeneous and heterogeneous sandpacks

Rock Samples: Tracer flow experiments were conducted on core plugs of 1.5 inch diameter and core samples of 3.5 inch diameter sample. First we described two of the experiments conducted on 1.5 inch diameter samples. Figure 8 and 9 show the effluent concentration and recovery efficiency plots for core samples 3V and 1H. The estimated value of flowing fraction for 3V sample is 0.5 and that for 1H sample is 0.2.

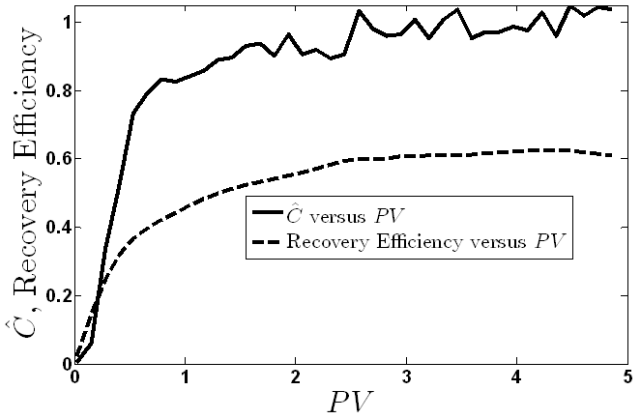

Figure 8. Effluent concentration and recovery efficiency for core plug 3V (diameter = 1.5 inch, length = 1.25 inch)

The estimated value of dispersivity for samples 3V and 1H is 1 cm and 0.8 cm respectively. However, the estimated value of mass transfer coefficient for both samples differs by one order of magnitude. To make better sense of the value of mass transfer coefficient, we express inverse of mass transfer coefficient in days. As seen from table 2, 1/M is 0.17 days for sample 3V while 0.02 days for sample 1H. We recall that T_2 relaxation spectrum for sample 1H has a continuous pore sizes distribution having vugs, small and intermediate size pores as shown in figure 4. Sample 3V on the other hand had did not have a continuous relaxation spectrum covering three orders of pore sizes. This could be the reason that sample 1H can have much higher value of mass transfer coefficient in comparison to sample 3V.

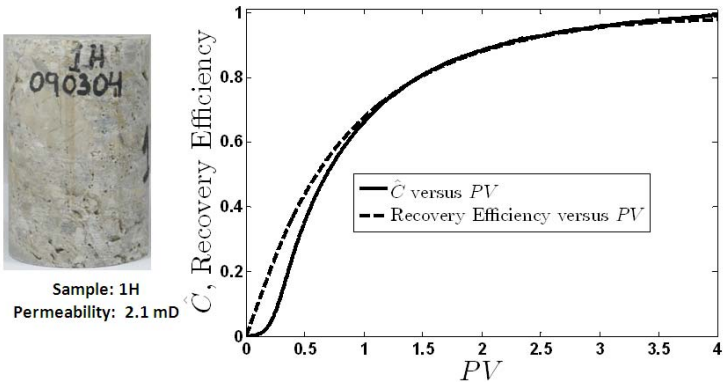

Figure 9. Effluent concentration and recovery efficiency for core plug 1H (diameter = 1.5 inch, length = 2.25 inch)

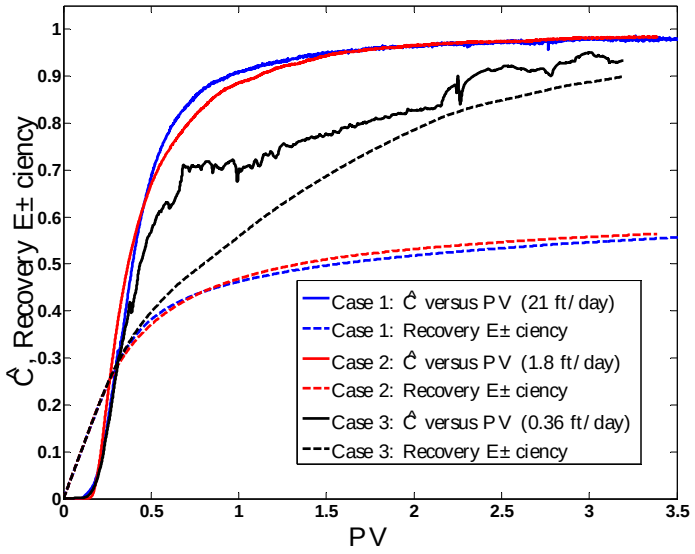

Figure 10. Effluent concentration and recovery efficiency for core plug 3.5 B (diameter 3.5 inch, length = 3.75 inch) at three different flowrates

Figure 10 shows the effect of displacement rates (interstitial velocity) on mass transfer between flowing and stagnant streams. Experiments were conducted for three different interstitial velocities (21 ft/day, 1.8 ft/day and 0.36 ft/day). As we reduced the interstitial velocity less than 1 ft/day, we begin to see significant mass transfer between flowing and stagnant streams as evidenced by enhanced recovery efficiency shown in figure 10.

After estimating unique model parameters from tracer flow experiments for a known sample, recovery efficiency can be calculated as a function of pore volume throughput for various displacement rates as shown in figure 11. We find that at high displacements rates only fraction of dead end pores is contacted and recovery is poor. As displacement rates are decreased we find the optimum rate at which recovery efficiency is significantly improved and reducing the displacement rates further are not useful. Experiments to characterize the pore structure in the laboratories should be conducted at flowrates which corresponds to $\mathbf{N_M}$ value of 1 or higher to ensure enough exchange between flowing and stagnant streams.

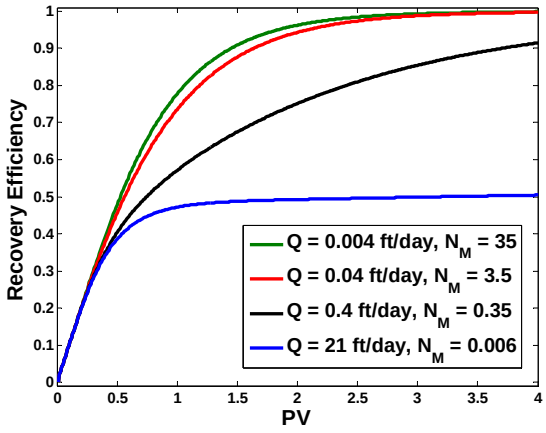

Figure 11. Estimated recovery efficient for various interstitial velocities using parameters estimated from tracer flow experiments.

DISCUSSION AND CONCLUSIONS

Calculated permeability for 3.5 inch diameter samples is in the range of 200-300 mD which is about two orders of magnitude higher than that for 1.5 inch diameter samples (0.5-6 mD). This proves our hypothesis that for such heterogeneous samples small diameter plugs of about 1 inch diameter are not suitable to study pore structure as the scale of heterogeneity is roughly the same order as the diameter of the plugs. Currently full sized cores are available only in 3.5 inch and 4.0 inch diameter sizes. Additional experiments will be conducted on 4.0 inch diameter samples to find out if 3.5 inch diameter samples are representative candidates for stydying connectivity of the vug systems.

Some inferences on the connectivity of the vugs can be made from NMR specturm alone. Spectrums such as in figure 4, showing overlap of different relaxation times with that for vugs may indicate possibility of the presence of connected pore network channels than the case when the different relaxation time peaks are well seperated. However such inferences should always be confirmed with other independent analysis such as Tracer flow experiments and thin section SEM images/CT scan micrographs.

Table 2 summarizes estimated values of flowing fraction, dispersivity and mass transfer coefficient for various core samples. For core samples of 1.5 inch diameter, we observe that flowing fraction is about 0.2-0.5. Flowing fraction is estimated to be 0.4 or higher for 3.5 inch diameter samples. In almost all samples, the value of dimensionless group for mass transfer ($\mathbf{N_M}$) is much smaller than 1. However for one 1.5 inch diameter core sample (1H) the estimated value of $\mathbf{N_M}$ is 5.3. The NMR T_2 relaxation time spectrum corresponding to this core sample is shown in figure 4. We observe that for this particular core sample NMR response shows a wide distribution of different pore sizes. Due to overlap of several pore sizes this core sample shows significantly higher value of mass transfer group ($\mathbf{N_M}$) than other core samples.

Table 2. Summary of estimated model parameters from various tracer flow experiments

Sample (ID)	**Diameter (inch)**	**f**	$\mathbf{N_M}$	$\mathbf{N_K}$	**v (ft/day)**	***α=K/v (cm)***	**1/M (day)**
3V	1.5	0.5	0.01	0.31	15	1.0	0.17
1H	1.5	0.2	5.3	0.14	1.7	0.8	0.02
3.5_A	3.5	0.39	0.05	0.23	3.1	2.2	2.54
3.5_B	3.5	0.47	0.34	0.183	0.36	1.7	2.45
3.5_C	3.5	0.71	0.13	0.19	0.4	1.8	6.03

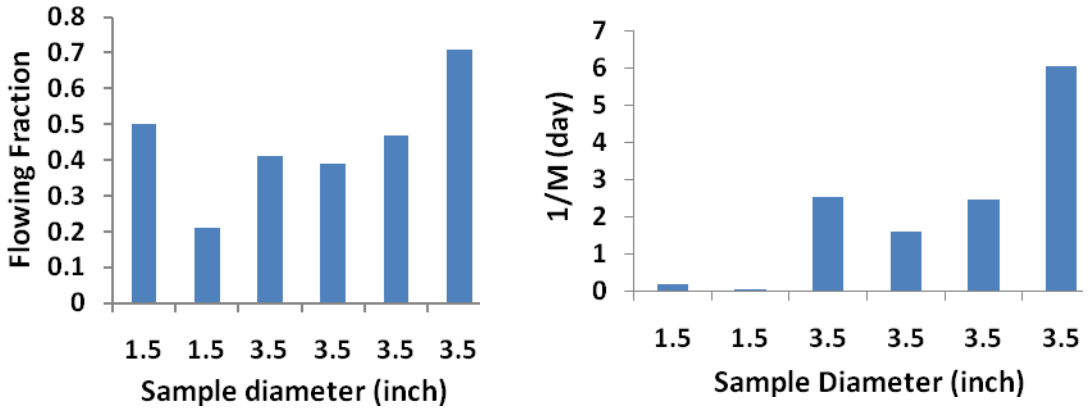

Figure 12. Bar charts showing flowing fraction and inverse of mass transfer coefficient estimated from tracer flow experiments

Estimated model parameters from tracer flow experiments are used to analyze different regimes of mass transfer. The regime of small mass transfer corresponds to the case when the value of dimensionless group for mass transfer is much smaller than unity ($N_M<1$). In this regime effluent concentration/recovery efficiency versus pore volume throughput curves are strongly dependent on interstitial velocity. The regime of strong mass transfer corresponds to the case when the value of dimensionless group for mass transfer is much greater than unity ($N_M > 1$). In the regime of strong mass transfer there is no dependence of insterstitial velocity on effluent concentration/recovery efficiency curve.

ACKNOWLEDGEMENTS

We acknowledge Petróleos Mexicanos (PEMEX) and Rice Consortium for processes in porous media for funding support.

REFERENCES

1. Palaz, I and Marfurt, K. 1997 *Carbonate seismology*. Society of Exploration Geophysicists
2. Chang, D., Vinegar, H., Morris, C. and Straley, C., "Effective Porosity, Producible Fluid, and Permeability in Carbonates from NMR Logging", The Log Analyst, 38, 1997, 60-72
3. Coats, K. H. and Smith, B. D. "Dead-End Pore Volume and Dispersion in Porous Media," *Soc. Pet. Eng. J., Trans., AIME,* (1964), 231, 73-84
4. Baker, L.E., Effects of dispersion and dead-end pore volume in miscible flooding. *Soc. Pet. Eng. J., Trans. AIME*, (1975), 263, 219-227
5. Brigham, W. "Mixing equations in short laboratory cores" Soc. Pet. Eng. 1974, J 14 91-99
6. Hollenbeck, K. INVLAP.m: "A matlab function for numerical inversion of Laplace transforms by the de Hoog algorithm" [Online; accessed 05-July-2009]. URL: http://www.isva.dtu.dk/staff/karl/invlap.m
7. Salter, S. J. and Mohanty, K. K. "Multiphase flow in porous media: I. Macroscopic observations and modeling", Paper SPE 11017 presented at 57th SPE Annual Technical Conference and Exhibition, New Orleans, LA, 1982
8. De Hoog, F., Knight, J. and Stokes, A. "An improved method for numerical inversion of Laplace transforms", *SIAM Journal on Scientific and Statistical Computing* 1975 **3** 357.
9. Marquardt, D. W. "An Algorithm for Least-Squares Estimation of Nonlinear Parameters", *Journal of the Society for Industrial and Applied Mathematics* 1963 **11** [No. 2] 31–441.